Proceedings World Geothermal Congress 2023
Beijing, China, September 15 – 17, 2023

An Innovative Concept of Regenerative Enhanced Geothermal Systems: A Field Case Study of The North German Basin

Muhammad Haris[a,b], Michael Zhengmeng Hou[a], Wentao Feng[c,d]

[a]Institute of Subsurface Energy Systems, Clausthal University of Technology, 38678 Clausthal-Zellerfeld, Germany

[b]Department of Petroleum & Gas Engineering, University of Engineering & Technology, 54890 Lahore, Pakistan

[c]College of Computer Science, Sichuan University, 610065 Chengdu, China

[d]Engineering Research Center of Machine Learning and Industry Intelligence, Ministry of Education, 610065 Chengdu, China

E-Mail: muhharis@hotmail.com (M. Haris), hou@tu-clausthal.de (M.Z. Hou), wtfeng2021@scu.edu.cn (W. Feng)

Keywords: Regenerative enhanced geothermal system, Hydraulic fracturing, Heat production, Electricity generation, Energy storage.

ABSTRACT

Geothermal energy is clean, renewable, efficient, independent of weather, and available in significant amounts. However, utilizing an effective approach has prime and foremost importance for the substantial exploitation of geothermal energy. In 2009, the GeneSys EGS project in the North German Basin was chosen to produce 2 MW of thermal energy to fulfill the residents' energy requirement. However, the low production rate and high-temperature decline caused the development of a salt plug inside the tubing due to cooling-induced precipitation. The salt plug was removed using the coil tubing technique; however, the high-temperature reduction (more than 50 ^{o}C) and extreme water salinity were major reasons for the project breakdown. The geothermal exploitation through GeneSys EGS using a single well with low flow rates could not provide acceptable results.

In this work, an innovative concept of a regenerative enhanced geothermal system is proposed, and the MHH-GeneSys region in the North German Basin is investigated for geothermal energy production as well as surplus renewable energy storage. Numerous thermo-hydro-mechanical coupled simulations have been conducted to obtain massive hydraulic fractures, and subsequently, heat and electricity potential have been forecasted. Multiple hydraulic fracturing results indicate that stress shadow considerably disturbs the subsequent fracture geometry, which ultimately alters the heat contribution of individual fractures. The energy production results show that the tendency of temperature decline in each fracture area increases with increased flow rate and well spacing. The total optimized installed power capacity of the whole projected EGS during 30 years drops from 14.34 MW to 10.16 MW, 10.66 MW to 7.04 MW and 7.17 MW to 4.14 MW for 288 L/s, 192 L/s and 96 L/s flow rate, respectively. The expected total cost of the multi-well multi-hydraulic fracture system is estimated at $ 120.47 million, having significant shares of drilling and operation & maintenance costs. The levelized cost of electricity (LCOE) is calculated at 0.0501 $/kWh, which is significantly economical. Moreover, after electricity production, the accumulated hot fluid can be used for direct heat applications. The high flow rates are beneficial in reducing the temperature reduction rate, leading to lower salt crystallization issues.

Lastly, to examine the surplus energy storage/recovery potential of the energy-depleted deep geothermal reservoir, continuous hot fluid injection/production cycles have been evaluated by adopting equal fluid volumes and time. It has been estimated that high energy recovery can be obtained by critically analyzing the continuous injection/production cycles. In addition, the stored energy can increase the life of the geothermal project by reducing the reservoir temperature reduction rate. The energy storage cycles can further help remove salt crystallization in wells.

1. INTRODUCTION

The economy and the world's population have resulted in an enormous demand for energy. Since the beginning of the 21st century, the total energy consumption has increased to 60 %. By the end of 2019, it has reached 581.1 exajoules (1 EJ = 10^{18} J), an increment of more than three times during the last fifty years. However, due to the Covid-19 pandemic in 2020, the world's energy consumption has declined to 4.5 %, the most significant decline ever recorded since World War II. Due to the imposition of lockdowns and limited transportation, the drop in oil consumption has been recorded as around three-quarters of the total decline in energy demand. Nevertheless, the energy demand is expected to rebound by 4.6 % in 2021-22 [1]. Due to the continuous decline in conventional petroleum resources, unconventional energy resources are currently playing an important role in meeting energy demands. However, fossil fuels are finite and non-renewable. Once fossil fuels have been produced through natural processes, replenishing them takes a

long time compared to the current consumption rate. In addition, these fuels are creating momentous complications for human health and the global climate. The energy from natural resources like sun, wind, hydro, and thermal from the earth's crust is categorized as renewable energy. It can replenish itself over a while without exhausting the earth's capital. Renewable energies emit no or low greenhouse gases and air pollutants, which are beneficial for the climate and human health. The exploitation of geothermal energy resources has fascinated general consideration due to its exceptional characteristics, like being stable, sustainable, clean, and independent of the weather. In addition, it is available for production for maximum working hours compared to other energy resources. Hot dry rock (HDR) resources with ultra-low porosity and permeability have been exploited through well-stimulation techniques and termed enhanced geothermal systems (EGSs) [2]. In EGS, cold fluid is injected through the injection well, and heated fluid is produced from the production well [3]. Within the depth of 10 km, more than 13 million exajoules (1 EJ = 10^{18} J) EGS resources have been estimated in the United States, of which 0.2 million EJ can be exploited through current technologies [2]. Multi-stage fracturing through a horizontal well is preferable to acquiring a larger stimulated reservoir volume (SRV) for geothermal exploitation. However, individual fracture configuration mainly depends on fracture spacing and the orientation of in-situ stresses. Numerous study results depict that the stress shadow greatly influences the middle fractures [4-6].

1.1 Research Objectives

The EGS project- GeneSys is in the North German Basin Hannover area with moderate temperatures ranging from 130 °C to 190 °C. This project aimed to produce 2 MW of thermal energy to meet the energy demands. A massive single hydraulic fracture was created by injecting 20,000 m^3 of fresh water having no proppant. The total acquired fracture area was 1.1 km^2. After six months, a substantial quantity of water was regained with a low flow rate. However, the recovered water was oversaturated with salt. The high-temperature reduction caused the formation of a salt plug inside the tubing due to cooling-induced precipitation. The salt plug was removed using the coil tubing technique; however, high-temperature reduction and extreme water salinity were major reasons for the project breakdown. This work proposes an innovative concept of a regenerative enhanced geothermal system. The MHH-GeneSys region in the North German Basin is investigated for geothermal energy production and surplus renewable energy storage (Figure 1). Furthermore, geothermal exploitation from multi-well multi-fracture systems can solve the salt production problem due to the continuous circulation of fluid. The state-of-the-art software FLAC3D^{plus} and TOUGH2MP-TMVOC are used to design the massive multi-fracture schemes in this area, as shown in Figure 2 while considering stress superposition effects. Correspondingly, the heat extraction performance for heat/electricity production and surplus energy storage is evaluated.

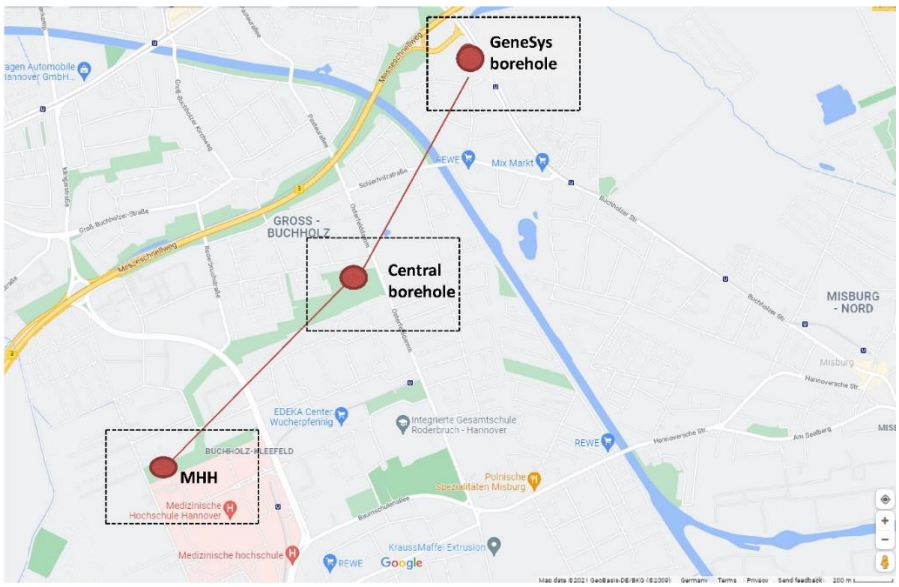

Figure 1: Overview of an innovative project area in Hannover (MHH-GeneSys-EGS).

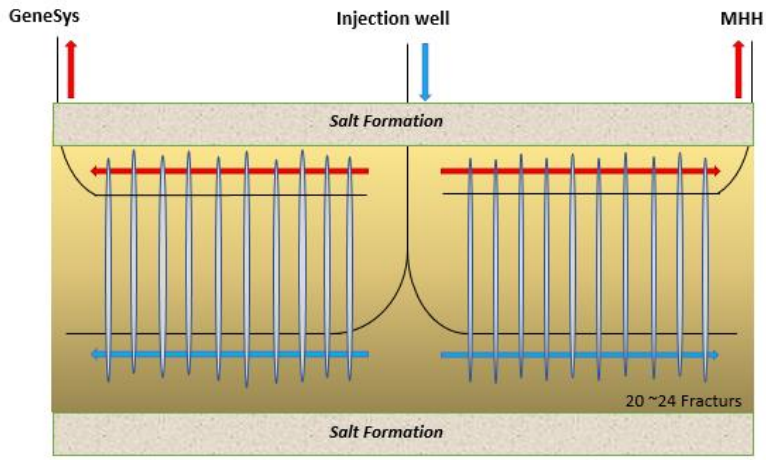

Figure 2: Schematic of the proposed multiple fracture pattern through multi-wells of water injection and production.

1.2 Simulation Concept

The thermo-hydro-mechanical (THM) coupled simulations have been performed using powerful simulators FLAC3D^{plus}-TOUGH2MP-TMVOC. The workflow of the numerical simulations is shown in Figure 3.

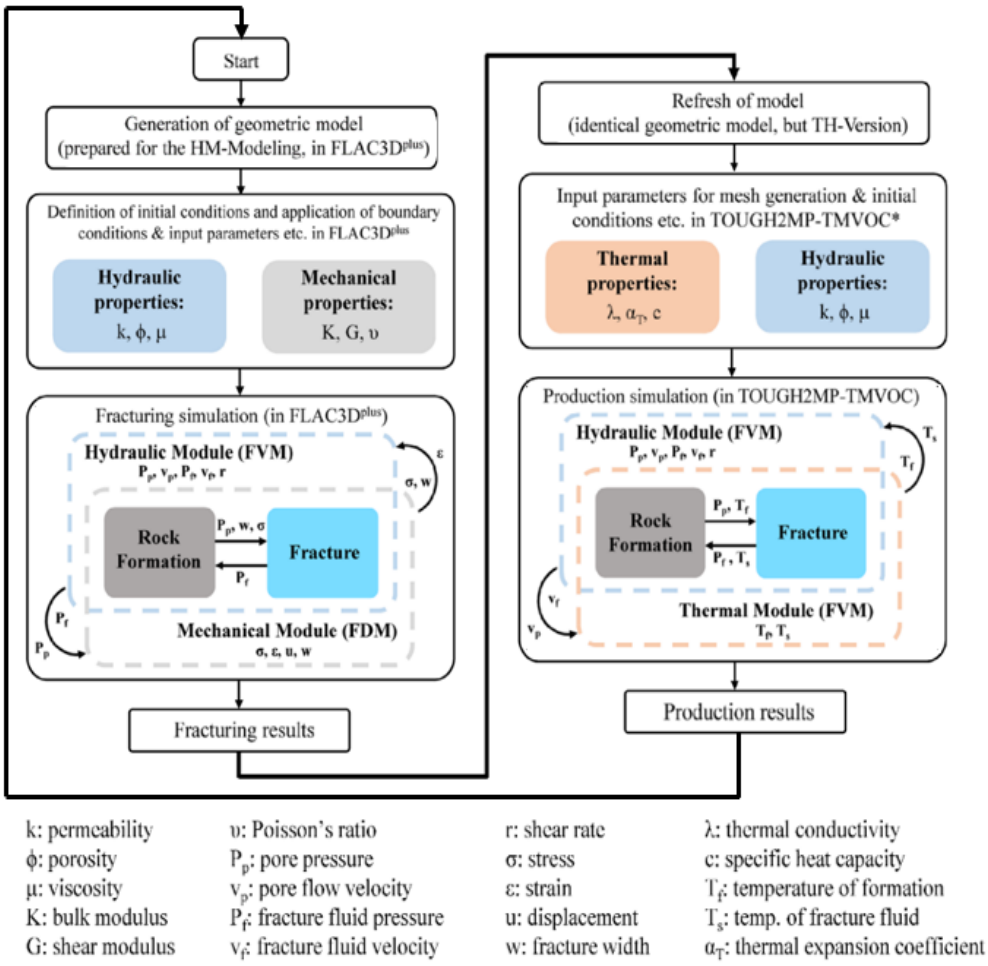

Figure 3: Flow chart of the computing scheme during the numerical modeling (modified from Haris et al. 2020 [6]).

The mechanical deformation that occurred due to the complex hydraulic fracturing process can be measured using the equation of motion (Eq. (1)), continuum equation (Eq. (2)), and constitutive equation (Eq. (3)).

$$\sigma_{ij,j} + \rho\left(b_i - \frac{dv_i}{dt}\right) = 0 \quad (1)$$

$$\Delta\varepsilon_{ij} = \frac{1}{2}\left(\Delta u_{i,j} + \Delta u_{j,i}\right) \quad (2)$$

$$\Delta\sigma' = D\Delta\varepsilon \quad (3)$$

where σ is the total stress [Pa], ρ is the rock density [kg/m^3], b_i is the volumetric acceleration [m/s^2], v_i is the rock mass velocity [m/s], t is the time [s], $\Delta\varepsilon$ is the strain increment [-], u is the displacement [m], $\Delta\sigma'$ is the effective stress increment [Pa], D is the physical matrix, i, j ϵ (x,y,z).

In addition, heat can be transmitted by different mechanisms. By integrating the heat flow equation (Eq. (4)), continuity equation (Eq. (5)), and thermal constitutive equation (Eq. (6)), the heat conduction process can be presented as in Eq. (7), while heat convection process can be described mathematically as in Eq. (8) [7].

$$q_i = -\lambda\frac{\partial T}{\partial i} \quad (4)$$

$$-\left(\frac{\partial q_x}{\partial x} + \frac{\partial q_y}{\partial y} + \frac{\partial q_z}{\partial z}\right) + q_v = \frac{\partial H}{\partial t} \quad (5)$$

$$\frac{\partial H}{\partial t} = \rho c_v \frac{\partial T}{\partial t} \quad (6)$$

$$\lambda\frac{\partial^2 T}{\partial x^2} + \lambda\frac{\partial^2 T}{\partial y^2} + \lambda\frac{\partial^2 T}{\partial z^2} + q_v = \rho c_v \frac{\partial T}{\partial t} \quad (7)$$

$$q_n = h(T_s - T_e) \quad (8)$$

where q_i is the heat flow in the i direction [W/m^2](i = x, y, z), λ is the rock thermal conductivity [W/(m·°C)], T is the rock temperature [°C], q_v is the heat source of volume [W/m^3], H is the stored heat per unit volume [J/m^3], ρ is the density [kg/m^3], c_v is the specific heat capacity [J/(kg·°C)]. q_n is the heat flux component normal to the boundary in the direction of the exterior normal [W/m^2], h is the convective heat-transfer coefficient [W/(m·°C)], T_s is the temperature at the surface of the solid body [°C], T_e is the temperature of the surrounding fluid [°C].

2. NUMERICAL MODELING (CASE STUDY)

A single massive fracture has been created using the engineering data of the GeneSys project, as provided by Hou et al. [8]. The modeling parameters have been verified through the fracturing results of Tischner et al. [9]. Figure 4 (a) shows a reasonable match between the simulated and calculated bottom hole pressures (BHP). After authentication, the ½ 3D geometric model has been generated, having multiple massive hydraulic fractures. The fractures are created sequentially, having a fracture spacing of 140 m (Figure 4 (b)). The injection rate and volume were kept the same for each fracture creation.

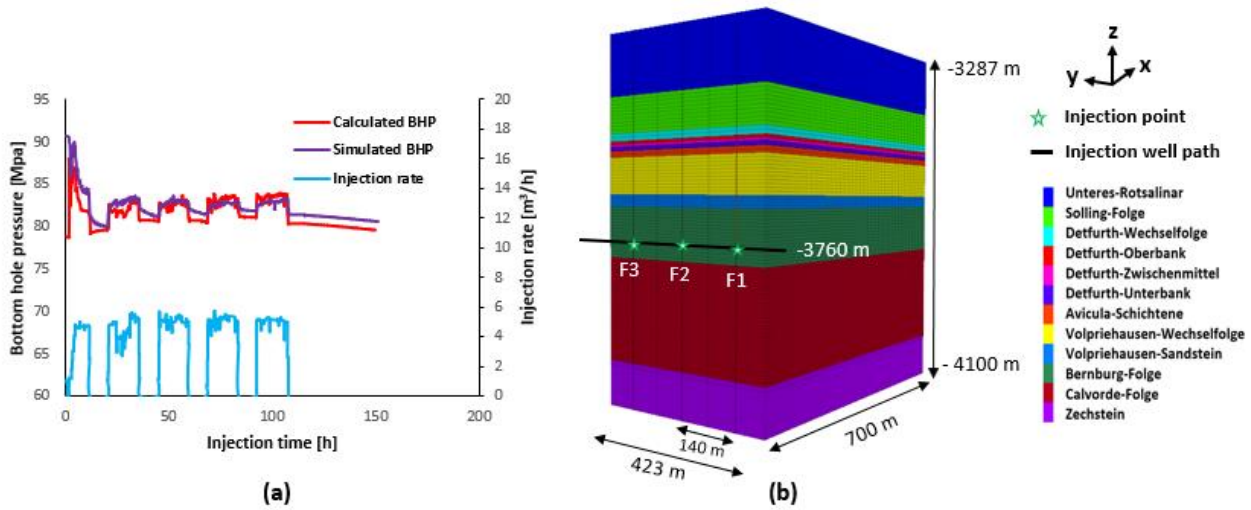

Figure 4: Schematic of (a) calculated and simulated BHP comparison for modeling verification, (b) 3D ½ model showing injection points of three fractures with 140 m fracture spacing.

Due to stress interference among the multiple fractures, different fracture configurations have been obtained, as shown in Figure 5. All the fractures have attained similar heights but with different widths and half lengths. It is observed that the variation in fracture widths of each fracture corresponds to the impact of stress shadow. In addition, each fracture geometry depends on the configuration of the previous fracture. Based on the fracturing results, 24 fractures are analyzed for energy production in this work.

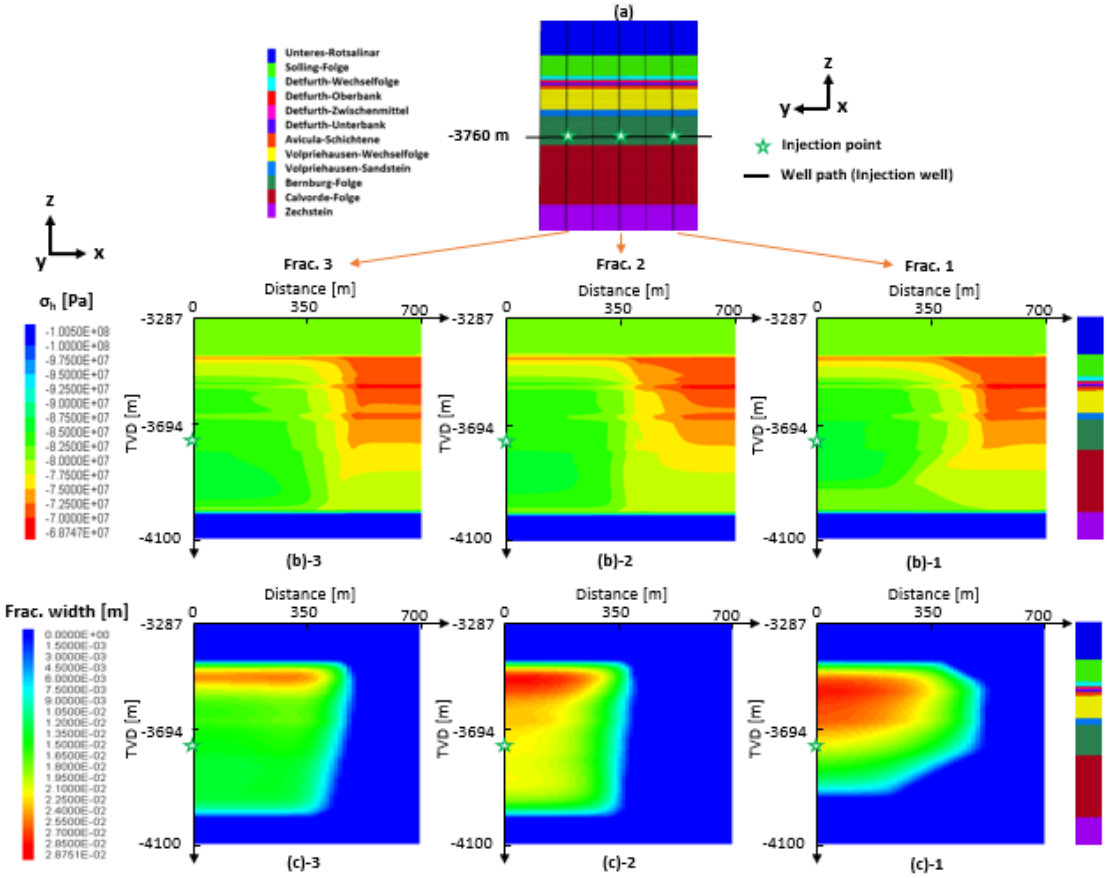

Figure 5: Representation of (a) 2D model, (b) minimum horizontal stress along three fracture planes, and (c) fracture widths with 140 m spacing.

2.1 Energy Production

After acquiring multiple hydraulic fracture configurations, geothermal energy is produced for 30 years. Water (at 60 ºC) is injected through a horizontal injection well, i.e., 3760 ft, at different flow rates and produced from the horizontal production well, i.e., 3500 ft depth, that passes through all multiple hydraulic fractures, as depicted in Figure 2. Figure 6 shows temperature decline comparison in fractures with different flow rates at the end of 30 years of injection/production time. The influence of increasing the flow rate on temperature depletion is somewhat perceptible. Higher flow rates are contributing to larger fractured areas in heat production.

The produced net energy can be calculated using the correlation Eq. (9) [10], and the geothermal heat capacity can be converted into electrical power using the relation described in Eq. (10) [11].

$$H = q\,(h_{\mathrm{o}} - h_{\mathrm{i}}) \tag{9}$$

$$W_{\mathrm{e}} = \eta\, W_{\mathrm{h}} \tag{10}$$

where q is the production rate [kg/s], h_o is the enthalpy of produced water [J/kg] and h_i is the enthalpy of injected water [J/kg], W_e is the electricity generation power [W], η is the conversion efficiency [-] and W_h is the heat production power [W].

The 10 % of conversion efficiency is adopted in this study for electricity power calculation [11-12]. The heat production power (W_h) for the 24-fracture system is decreasing from 143.4 MW_t to 101.6 MW_t for 288 L/s, 106.6 MW_t to 70.4 MW_t for 192 L/s, 71.7 MW_t to 41.4 MW_t, during 30 years of production. Therefore, electricity generation power (W_e) decreases from 14.34 MW to 10.16 MW, 10.66 MW to 7.04 MW, and 7.17 MW to 4.14 MW for 288 L/s, 192 L/s, and 96 L/s, respectively, as shown in Figure 7. In addition, the cumulative energy produced in 30 years is estimated at 1070 GWh, 1750 GWh, and 2400 GWh for 96 L/s, 192 L/s, and 288 L/s, respectively.

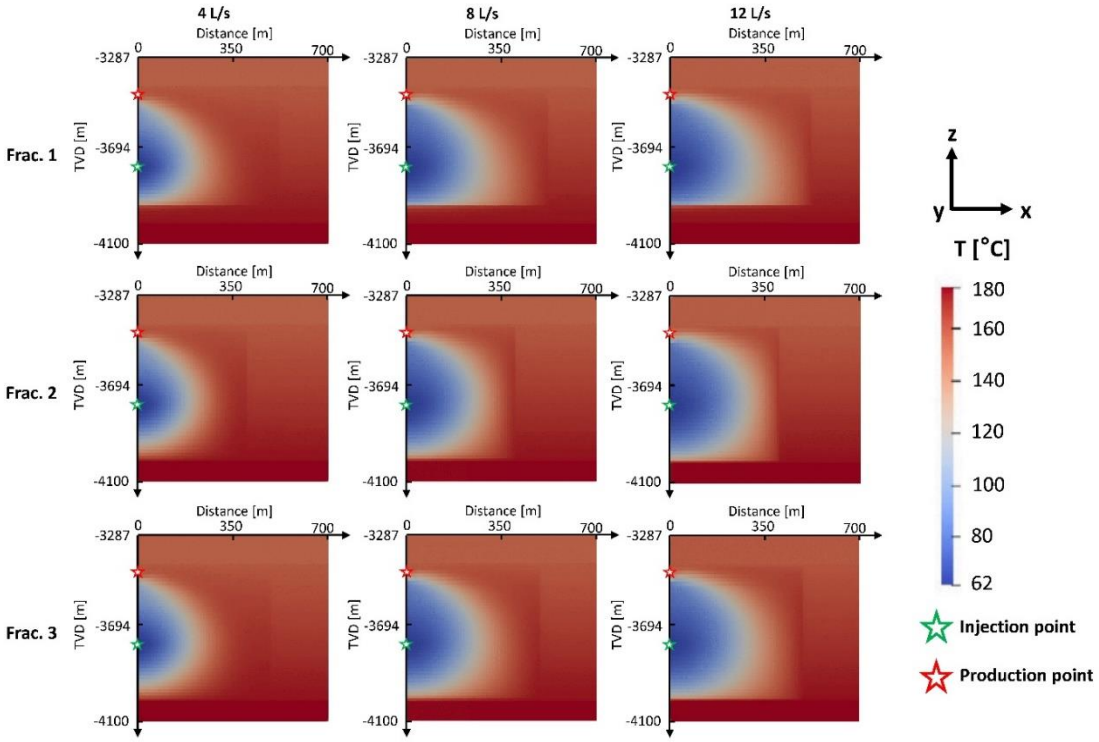

Figure 6: Comparison of temperature decline in fracture planes after 30 years of production with different flow rates per fracture.

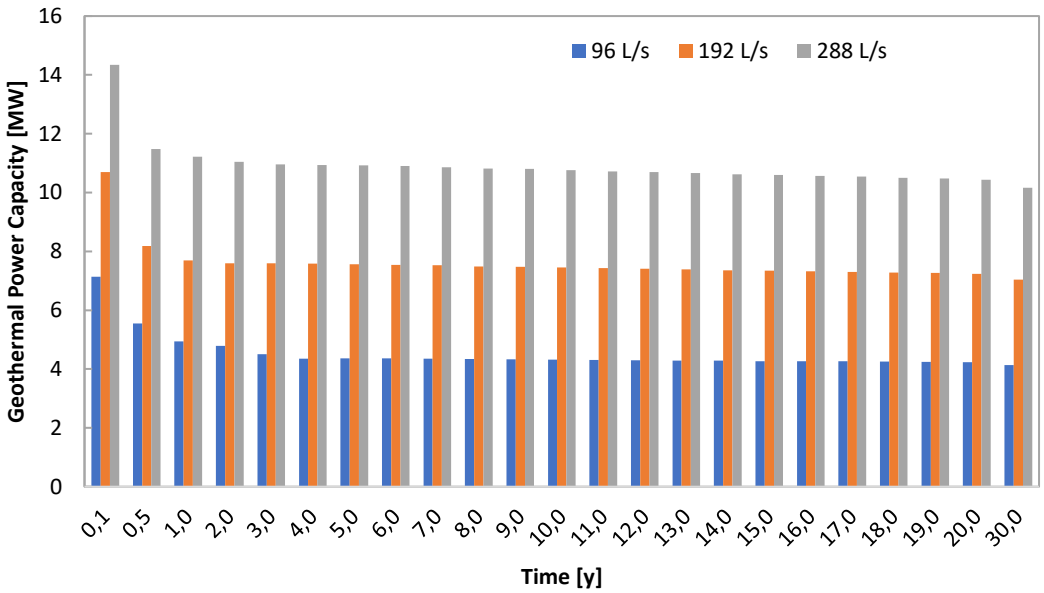

Figure 7: Comparative energy production results through different flow rates

2.2 Energy Storage

The deployment of underground heat storage is a necessity of the recent era. It can temporarily store surplus energy and decrease peak loads with intelligent waste energy management. The massive multiple fractured models of the MHH-GeneSys site that have been used initially for geothermal energy production are further investigated for surplus renewable energy storage and recovery. This study evaluates energy storage efficiency using a recovery factor, defined as the ratio of recovered energy to stored energy concerning ambient reservoir temperature when an equal amount of water is injected and produced [13-14]. The zero-recovery factor means none of the stored energy is recovered or produced, and the increase in the recovery factor will decrease the storage efficiency and vice versa. The heat loss in the borehole is assumed as negligible. The injection/production cycles have been analyzed by adopting equal fluid volume and time without pause. For example, in the case of the monthly cycle, hot water (at 200 °C) is injected through each

well that flow inside the fracture at a constant injection rate. Afterward, the injected fluid is produced from wells for one month. During five injection/production cycles for the 24-fracture pattern, produced net energy increases from 140 TJ to 178 TJ, 442 TJ to 519 TJ, and 924 TJ to 991 TJ for monthly, quarterly, and semi-annually cycles, respectively. In contrast, stored energy declines gradually after every cycle, particularly for the short cyclic period compared to the longer cyclic period. These results are presented in Figure 8 for monthly, quarterly, and semi-annual periods.

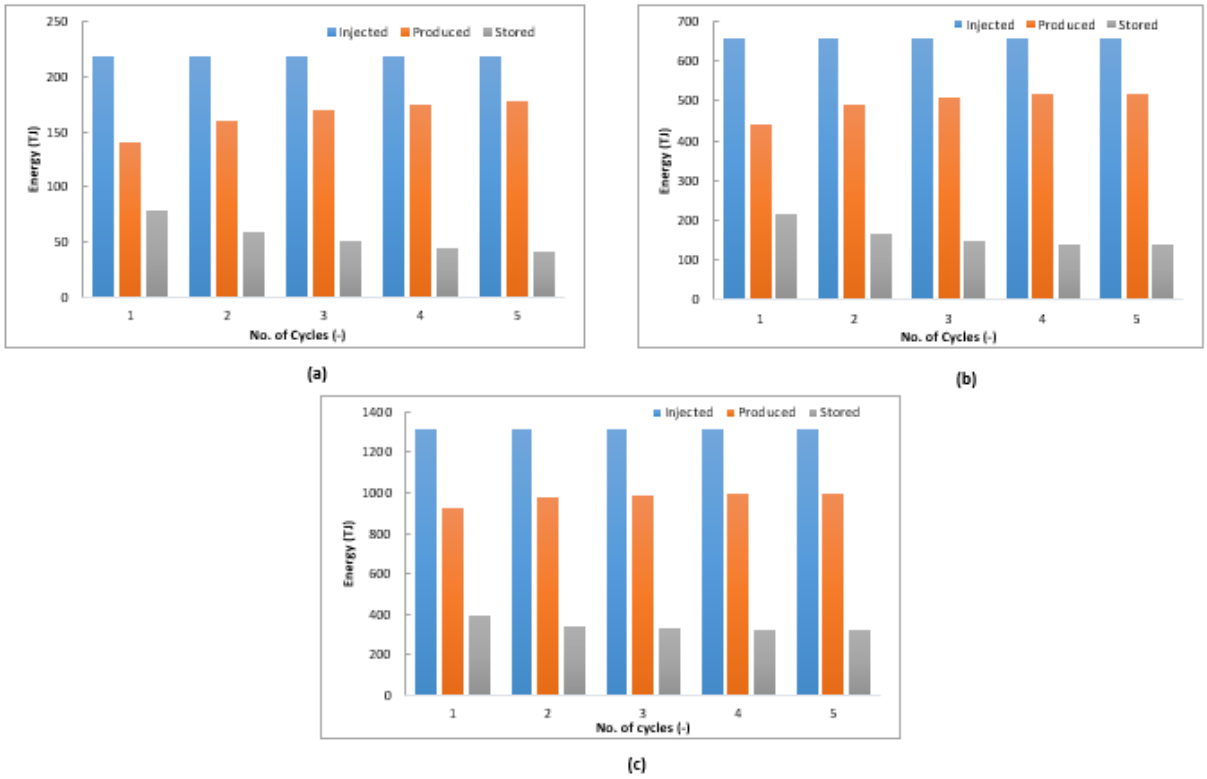

Figure 8: Comparative energy results during injection/production operations for (a) monthly, (b) quarterly, and (c) semi-annual cycles.

Figure 9 shows the production temperature profile during the injection and production stages for five years. It is observed that the temperature rises after every cycle. However, an increase in the rate of temperature decreases after every cycle. After several cycles, no significant change in temperature is observed, which depicts that the reservoir is achieving temperature equilibrium. Furthermore, it is noticed that the number and duration of injection/production cycles are essential features that can considerably affect recovery and storage efficiency. Due to the increased reservoir temperature, the fractured EGS is again available for geothermal energy exploitation.

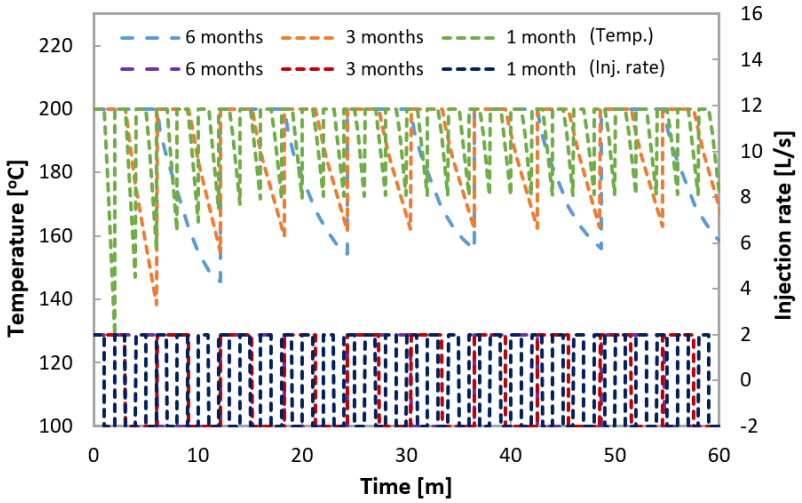

Figure 7: Temperature profile at injection/production points during five years for different time cycles.

2.3 Cost Evaluation

In conventional hydrothermal systems, in-situ fluid is produced from the production without excessive drilling and fracturing operations. On the contrary, EGS systems typically involve the injection/production of water or any suitable fluid at higher depths to come across the higher rock temperature along with fracturing operations. Due to these reasons, the cost of an EGS project is relatively high. Although high inflation rate and fuel prices at present hinder the exact cost calculation, a basic framework of cost evaluation helps in better feasibility of cost in the future. Therefore, the cost evaluation has been conducted by adopting a simplified approach that defines the levelized cost of electricity (LCOE). The LCOE can be calculated by dividing the total investment cost by the total power generation [15].

$$\text{LCOE} = \frac{Total\ Investment\ Cost}{Total\ Power\ Generation} \tag{11}$$

Three major classifications contribute to the investment cost of an EGS project, i.e., surface costs, subsurface costs, and operation and maintenance costs (O&M). The cost analysis has been performed by analyzing some cases published in the literature. Lei et al. [16] estimated the exploration cost of about $ 4.5 million for the Qiabuqia geothermal field in China. For the proposed EGS power plant having a 3 MW capacity in the Daqing oilfield China, the surface installation cost was expected to be $ 6 million [11]. The surface installation costs of five power plants in Iceland were estimated to be 1000 $/kW for the power plant ranging from 20-60 MW, and it was concluded that the surface equipment cost varies linearly with plant size [17]. However, unit capital cost decreases exponentially with increased power capacity due to economy of scale. More precisely, it varies from 2000 $/kW for a 5 MW power plant to 1000 $/kW for a 150 MW power plant [11, 18]. Therefore, the total surface cost based on installed geothermal power capacity can be calculated using Eq. (12).

$$C_{surf} = C_{exp} + 2000 * P_t \tag{12}$$

where C_{surf} is the surface cost [$], C_{exp} is the exploration cost [$], P_t is the installed power capacity [MW].

In the case of subsurface costs, the highest ambiguity in cost calculations exists due to higher uncertainties. Oil and gas rigs are often utilized for geothermal projects with certain modifications. These modifications are made to encounter much harder and more abrasive geothermal rocks than sedimentary formations. The situation may worsen for abnormal subsurface conditions such as under-pressured formations, which may lead to high fluid leak-off and contribute 10-20 % of the well cost. Moreover, an increased number of casing strings causes longer drilling time than hydrocarbon well completion [11]. Therefore, it is challenging to calculate the drilling cost accurately. Zang et al. [11] estimated the cost of one drilling well at $ 15 million for about 7500 m hole section. Whereas $ 5 million could be saved using an abandoned well in the same field. The assessment of MIT (Massachusetts Institute of Technology) in 2004 suggested the drilling cost of about $ 13.3 million in Clear Lake country for a 6 km well length with six casing strings [19]. Lei et al. [16] estimated the drilling cost of about 9.36 million for three wellbore sections. In addition, the logging and single fracturing costs have been estimated at $ 0.45 million for each operation for China's Qiabuqia geothermal field. Operations and maintenance (O&M) costs are related with the costs occurred during the reservoir exploitation phase. For higher production capacity reservoirs, O&M costs decreases exponentially, i.e., from 20 $/MWh to 14 $/MWh for 5 MW and 150 MW plant capacity, respectively [16,18]. It can be estimated using Eq. (13) in $/MWh.

$$C_{O\&M} = 20 \exp(-0.0025\ (P_t - 5)) \tag{13}$$

According to our simulation results of 288 L/s flow rate, the LCOE is calculated for the average plant capacity of 12.2 MW. Therefore, O&M costs are estimated to be 19.64 $/MWh. Based on previous studies, the three wells' drilling cost, which covers the vertical and horizontal sections, is estimated to be $ 30 million. In addition, exploration, logging, and hydraulic fracturing costs are estimated to be $ 9 million, $ 0.9 million, and $ 9 million, respectively. Therefore, drilling, stimulation, logging, and exploration costs are estimated at $ 48.9 million. While mentioning all expected geothermal power plant costs above, the total cost is calculated using Eq. (14).

$$C_{total} = 48.9 + 2000 * P_t + W_t * C_{O\&M} \tag{14}$$

where Wt is total power generation in 30 years [GWh].

The LCOE for 288 L/s flow rate through 24 hydraulic fractures is calculated at 0.0501 $/kWh, which is quite economical.

3. CONCLUSION

This work proposes an innovative concept of a regenerative enhanced geothermal system that integrates geothermal energy production and surplus energy storage in massive multiple hydraulic fractures. The state-of-the-art software FLAC3D^{plus} and TOUGH2MP-TMVOC are used to perform THM-coupled simulations. Based on our results, the following conclusions have been attained.

- The incorporation of stress shadow effects on individual fracture geometry can provide realistic energy production results compared to identical fracture geometry assumptions.
- The impact of flow rate on energy production through the proposed wells' arrangement is vital. The flow rates should be comparable with the total multiple hydraulic fractured areas to achieve optimized energy production.
- The electric power capacity for the MHH-GeneSys area using 288 L/s flow rate decreases from 14.34 MW to 10.16 MW through a 24-fracture configuration that meets the commercial requirements, and the LCOE is estimated at 0.0501 $/kWh, which is quite economical.
- The surplus energy storage results show that a regenerative EGS could develop as the formation temperature rises after every cycle. In this way, the surplus energy can be stored efficiently and keep a geothermal reservoir more renewable by reducing the reservoir temperature reduction rate.

REFERENCES

[1]. "Global Energy Review 2021," p. 36, 2021.

[2]. J. W. Tester *et al.*, "Impact of enhanced geothermal systems on US energy supply in the twenty-first century," *Philos Trans A Math Phys Eng Sci*, vol. 365, no. 1853, pp. 1057–1094, Apr. 2007, doi: 10.1098/rsta.2006.1964.

[3]. R. A. Crooijmans, C. J. L. Willems, H. M. Nick, and D. F. Bruhn, "The influence of facies heterogeneity on the doublet performance in low-enthalpy geothermal sedimentary reservoirs," *Geothermics*, vol. 64, pp. 209–219, Nov. 2016, doi: 10.1016/j.geothermics.2016.06.004.

[4]. J. E. Olson, "Multi-fracture propagation modeling: Applications to hydraulic fracturing in shales and tight gas sands," presented at the The 42nd U.S. Rock Mechanics Symposium (USRMS), Jun. 2008. Accessed: Mar. 05, 2021. [Online]. Available: https://onepetro.org/ARMAUSRMS/proceedings/ARMA08/All-ARMA08/ARMA-08-327/119244.

[5]. N. P. Roussel and M. M. Sharma, "Optimizing Fracture Spacing and Sequencing in Horizontal-Well Fracturing," *SPE Production & Operations*, vol. 26, no. 02, pp. 173–184, May 2011, doi: 10.2118/127986-PA.

[6]. M. Haris, M. Z. Hou, W. Feng, J. Luo, M. K. Zahoor, and J. Liao, "Investigative Coupled Thermo-Hydro-Mechanical Modelling Approach for Geothermal Heat Extraction through Multistage Hydraulic Fracturing from Hot Geothermal Sedimentary Systems," *Energies*, vol. 13, no. 13, Jan. 2020, doi: 10.3390/en13133504.

[7]. W. Feng, P. Were, M. Li, Z. Hou, and L. Zhou, "Numerical study on hydraulic fracturing in tight gas formation in consideration of thermal effects and THM coupled processes," *Journal of Petroleum Science and Engineering*, vol. 146, pp. 241–254, Oct. 2016, doi: 10.1016/j.petrol.2016.04.033.

[8]. Z. Hou, T. Kracke, L. Zhou, and X. Wang, "Gebirgsmechanische Auswirkungen von Fracs im tiefen Untergrund des Norddeutschen Beckens: geologische Steinsalzbarriereintegrität und maximale Magnitude induzierter Mikrobeben anhand der GeneSys-Stimulation im Mai 2011 = Rock mechanical influences of hydraulic fracturing deep underground the North German Basin: geological integrity of the cap rock salt and maximum magnitude of induced microseismicity based on the GeneSys stimulation in May 2011," *Erdöl Erdgas Kohle*, vol. 11, pp. 454–460, Jan. 2012.

[9]. T. Tischner *et al.*, "Massive Hydraulic Fracturing in Low Permeable Sedimentary Rock in the GeneSys Project," p. 11, 2013.

[10]. J.B. Randolph, M.O. Saar, "Coupling carbon dioxide sequestration with geothermal energy capture in naturally permeable, porous geologic formations: implications for CO2 sequestration," *Energy Proc.* 4 (2011) 2206–2213, Jan, https://doi.org/10.1016/j.egypro.2011.02.108.

[11]. Y.-J. Zhang, Z.-W. Li, L.-L. Guo, P. Gao, X.-P. Jin, and T.-F. Xu, "Electricity generation from enhanced geothermal systems by oilfield produced water circulating through reservoir stimulated by staged fracturing technology for horizontal wells: A case study in Xujiaweizi area in Daqing Oilfield, China," *Energy*, vol. 78, pp. 788–805, Dec. 2014, doi: 10.1016/j.energy.2014.10.073.

[12]. S. J. Zarrouk and H. Moon, “Efficiency of geothermal power plants: A worldwide review,” *Geothermics*, vol. 51, pp. 142–153, Jul. 2014, doi: 10.1016/j.geothermics.2013.11.001.

[13]. B. Drijver, M. van Aarssen, and B. de Zwart, “High-temperature aquifer thermal energy storage (HT-ATES): sustainable and multi-usable,” p. 10, 2012.

[14]. W. T. Sommer *et al.*, “Thermal performance and heat transport in aquifer thermal energy storage,” *Hydrogeol J*, vol. 22, no. 1, pp. 263–279, Feb. 2014, doi: 10.1007/s10040-013-1066-0.

[15]. T. Xu, et al., “Prospects of power generation from an enhanced geothermal system by water circulation through two horizontal wells: a case study in the Gonghe Basin, Qinghai Province, China,” *Energy* 148 (Apr. 2018) 196–207, https://doi.org/10.1016/j.energy.2018.01.135.

[16]. Z. Lei, et al., “Electricity generation from a three-horizontal-well enhanced geothermal system in the Qiabuqia geothermal field, China: slickwater fracturing treatments for different reservoir scenarios,” *Renew. Energy* 145 (Jan. 2020) 65–83, https://doi.org/10.1016/j.renene.2019.06.024.

[17]. V. Stefánsson, “Investment cost for geothermal power plants,” *Geothermics*, vol. 31, no. 2, pp. 263–272, Apr. 2002, doi: 10.1016/S0375-6505(01)00018-9.

[18]. C. R. Chamorro, M. E. Mondéjar, R. Ramos, J. J. Segovia, M. C. Martín, and M. A. Villamañán, “World geothermal power production status: Energy, environmental and economic study of high enthalpy technologies,” *Energy*, vol. 42, no. 1, pp. 10–18, Jun. 2012, doi: 10.1016/j.energy.2011.06.005.

[19]. J. W. Tester, B. Livesay, B. J. Anderson, M. C. Moore, and et al, “The Future of Geothermal Energy – Impact of Enhanced Geothermal Systems (EGS) on the United States in the 21st Century,” *An assessment by an MIT-led interdisciplinary panel*, p. 372, 2006.